

Provided for non-commercial research and education use.
Not for reproduction, distribution or commercial use.



This article appeared in a journal published by Elsevier. The attached copy is furnished to the author for internal non-commercial research and education use, including for instruction at the authors institution and sharing with colleagues.

Other uses, including reproduction and distribution, or selling or licensing copies, or posting to personal, institutional or third party websites are prohibited.

In most cases authors are permitted to post their version of the article (e.g. in Word or Tex form) to their personal website or institutional repository. Authors requiring further information regarding Elsevier's archiving and manuscript policies are encouraged to visit:

<http://www.elsevier.com/copyright>

Available online at www.sciencedirect.com

SciVerse ScienceDirect

www.elsevier.com/locate/jmbbm

Deformation behavior and mechanical properties of amyloid protein nanowires

Max Solar^{a,b}, Markus J. Buehler^{a,c,d,*}

^aLaboratory for Atomistic and Molecular Mechanics (LAMM), Department of Civil and Environmental Engineering, Massachusetts Institute of Technology, 77 Massachusetts Ave., Cambridge, MA 02139, USA

^bDepartment of Materials Science and Engineering, Massachusetts Institute of Technology, 77 Massachusetts Ave., Cambridge, MA 02139, USA

^cCenter for Computational Engineering, Massachusetts Institute of Technology, 77 Massachusetts Ave., Cambridge, MA 02139, USA

^dCenter for Materials Science and Engineering, Massachusetts Institute of Technology, 77 Massachusetts Ave., Cambridge, MA 02139, USA

ARTICLE INFO

Article history:

Received 14 May 2012

Received in revised form

3 October 2012

Accepted 9 October 2012

Available online 28 November 2012

Keywords:

Amyloid

Mechanics

Multiscale

Hierarchical

Deformation

Failure

Toughness

Stiffness

ABSTRACT

Amyloid fibrils are most often associated with their pathological role in diseases like Alzheimer's disease and Parkinson's disease, but they are now increasingly being considered for uses in functional engineering materials. They are among the stiffest protein fibers known but they are also rather brittle, and it is unclear how this combination of properties affects the behavior of amyloid structures at larger length scales, such as in films, wires or plaques. Using a coarse-grained model for amyloid fibrils, we study the mechanical response of amyloid nanowires and examine fundamental mechanical properties, including mechanisms of deformation and failure under tensile loading. We also explore the effect of varying the breaking strain and adhesion strength of the constituent amyloid fibrils on the properties of the larger structure. We find that deformation in the nanowires is controlled by a combination of fibril sliding and fibril failure and that there exists a transition from brittle to ductile behavior by either increasing the fibril failure strain or decreasing the strength of adhesion between fibrils. Furthermore, our results reveal that the mechanical properties of the nanowires are quite sensitive to changes in the properties of the individual fibrils, and the larger scale structures are found to be more mechanically robust than the constituent fibrils, for all cases considered. More broadly, this work demonstrates the promise of utilizing self-assembled biological building blocks in the development of hierarchical nanomaterials.

© 2012 Elsevier Ltd. All rights reserved.

1. Introduction

Amyloid fibrils are a class of misfolded proteins that have garnered much interest lately because of their pathological role in neurodegenerative diseases such as Alzheimer's disease and Parkinson's disease (Dobson, 1999, 2003; Knowles and Buehler, 2011). In addition to their role in disease,

though, amyloids are also exploited in nature for functional roles, and their mechanical and adhesive properties and propensity to self-assemble make them a promising building block for use in hierarchically assembled nanomaterials (Fig. 1(a)) (Chapman et al., 2002; Chiti and Dobson, 2006; Fowler et al., 2007; Knowles and Buehler, 2011; Maji et al., 2009; Zhang, 2003). Some progress has been made in the

*Corresponding author at: Department of Civil and Environmental Engineering, Massachusetts Institute of Technology, Cambridge, MA 02139, United States.

E-mail address: mbuehler@mit.edu (M.J. Buehler).

development of protein based materials and structures, including some made with amyloid fibrils, but only limited mechanical characterization has been performed and the underlying deformation mechanisms that control the behavior of these materials remains largely unexplored (Knowles et al., 2007, 2010; Knowles and Buehler, 2011; Kol et al., 2005; Zhang, 2003; Zhang et al., 1993).

The underlying structure of amyloid fibrils comprises a dense hydrogen-bonded network that results in β -sheets that extend the length of the fibril (Dobson, 1999, 2003; Jaroniec et al., 2004; Luhrs et al., 2005; Sawaya et al., 2007). This secondary structure makes amyloid fibrils among the stiffest protein materials known; previous computational and experimental work has consistently shown that their Young's modulus can be as high as 10–30 GPa (Knowles et al., 2007; Kol et al., 2005; Paparcone and Buehler, 2010, 2011; Paparcone et al., 2010b; Smith et al., 2006; Solar and Buehler, 2012; Xu et al., 2010). However, amyloid fibrils are also quite brittle, and they become more brittle as their length is increased (Paparcone and Buehler, 2011). This feature is found to have a profound effect on the growth kinetics of amyloid fibrils (Aguzzi, 2009; Collins et al., 2004; Shorter and Lindquist, 2006; Tanaka et al., 2006). What is still unclear is the extent to which the intrinsic brittleness of amyloids at the fibril scale affects properties at larger length scales; it is very important to have a clear understanding of this in order to further the development of *de novo* materials based on amyloid fibrils. Specifically, will assemblies of amyloid fibrils in films, plaques or wires have useful mechanical properties in spite of the intrinsic brittleness of their constituents? The natural existence of amyloid-based adhesives suggests that mechanically useful properties emerge, but the mechanism by which this occurs remains unclear.

In the present work we employ a simple model to systematically study the deformation behavior and mechanical response of a nanowire structure composed of amyloid fibrils. Much theoretical work has been performed on similar geometries including bundles of carbon nanotubes, and it was shown that the properties of the bundle structures depend greatly on the properties of the constituent nanotubes (which vary due to both geometry and the presence of defects) (Pugno, 2007a, b, 2010). While the nanowire studied here is a relatively simple structure, it can provide key insight into the dominant deformation mechanisms and elucidate trends that emerge upon varying the properties of the constituent amyloid fibrils. By varying both the fibril failure strain and the strength of adhesion between fibrils (mimicking different solvent conditions and amino acid sequence variations), we explore how the use of such brittle building blocks affects the mechanical response of larger scale structures, and examine the extent to which new deformation pathways that exist in these structures can effectively mitigate the brittleness of the amyloid fibrils.

2. Methods

2.1. Mesoscale bead spring model

A coarse-grain model is used to enable the exploration of the mechanical response of amyloid structures that are beyond the

size scale accessible with a fully atomistic description. Individual amyloid fibrils are described by a simple bead-spring model as described in a series of earlier papers (Paparcone et al., 2010a, 2011). In this model three layers of the β -sheet structure of the amyloid fibril are represented by a single bead with an inter-bead separation of 1.272 nm; all parameters in that model were identified from full-atomistic simulations. The total energy of the system is given by $E_{total} = E_{bond} + E_{angle} + E_{adhesion}$, where E_{bond} describes the axial deformation of the individual fibrils, E_{angle} describes the bending deformation of the fibrils, and $E_{adhesion}$ describes the interfibril adhesion.

The amyloid fibrils studied in this work feature a stiffening behavior in both compression and tension. For small deformation the elastic modulus is 2.34 GPa but for compressive strains exceeding 0.1% and tensile strains exceeding 0.2%, the modulus increases to 12.43 GPa and 18.05 GPa, respectively (Paparcone et al., 2010b). To account for this behavior, the bonding energy is described by $E_{bond} = \sum_{bonds} \phi_b$ and the energy between bonded pairs of beads is given by

$$\phi_b = \frac{1}{2} \begin{cases} k_b^s (r_{stiff}^c - r_0)^2 + k_b^c (r - r_{stiff}^c)^2, & r \leq r_{stiff}^c \\ k_b^s (r - r_0)^2, & r_{stiff}^c < r < r_{stiff}^t \\ k_b^s (r_{stiff}^t - r_0)^2 + k_b^t (r - r_{stiff}^t)^2, & r_{stiff}^t \leq r \leq r_{break} \\ k_b^s (r_{stiff}^t - r_0)^2 + k_b^t (r_{break} - r_{stiff}^t)^2, & r > r_{break} \end{cases} \quad (1)$$

The parameters k_b^i are the spring constants for the relevant strain ranges (c for compression, t for tension, and s for small strain) and are parameterized so that the fibrils have the moduli given above. The bending behavior of the amyloid fibrils is described by a harmonic angle potential; the total bending energy is given by $E_{angle} = \sum_{angles} \phi_a$, where $\phi_a = 1/2 k_\theta (\theta - \theta_0)^2$.

A Lennard-Jones potential is used to model the interfibril adhesion where $E_{adhesion} = \sum_{pairs} \phi_{LJ}$ with $\phi_{LJ} = 4A[(B/r)^{12} - (B/r)^6]$.

All amyloid fibrils studied in this work have an initial length of 100 nm, and the nominal values of all parameters are given in Table 1. The parameters used are specific to the A β (1–40) amyloid fibril, but the model can be easily changed to describe any number of other amyloid or similar protein fibrils. This mesoscale model is implemented in the LAMMPS code (Plimpton, 1995).

2.2. Nanowire assembly and nanomechanical characterization

To create the amyloid nanowire geometry used in this study, 100 coarse-grain amyloid fibrils, each 100 nm long, are randomly positioned along the nanowire axis. The fibrils are oriented along a random angle within 30 degrees of the fibril axis in both transverse directions, and the ends of the fibrils are placed within 10 Å of the nanowire axis. Energy minimization is performed to bring the fibrils together into a single structure followed by equilibration to eliminate any residual stress. Fig. 1(b) shows images of both the starting configuration with randomly oriented fibrils as well as the equilibrated structure. The initial length of the amyloid nanowire structure is approximately 575 nm.

Table 1 – Summary of mesoscopic parameters for the A β (1–40) amyloid fibril model.

Parameter	Units	Nominal value
Stiffness in small strain, k_b^s	kcal mol ⁻¹ Å ⁻²	18.72
Stiffness in compression, k_b^c	kcal mol ⁻¹ Å ⁻²	99.42
Stiffness in tension, k_b^t	kcal mol ⁻¹ Å ⁻²	144.37
Bending stiffness, k_θ	kcal mol ⁻¹	4369.8
Equilibrium bead spacing, r_0	Å	12.72
Bead spacing for onset of stiffening in compression, r_{stiff}^c	Å	12.70
Bead spacing for onset of stiffening in tension, r_{stiff}^t	Å	12.75
Bead spacing for bond breaking, r_{break}	Å	12.78
Equilibrium angle, θ_0	Deg	180
LJ parameter, A	kcal mol ⁻¹ Å ⁻¹	27.94
LJ parameter, B	Å	38.15

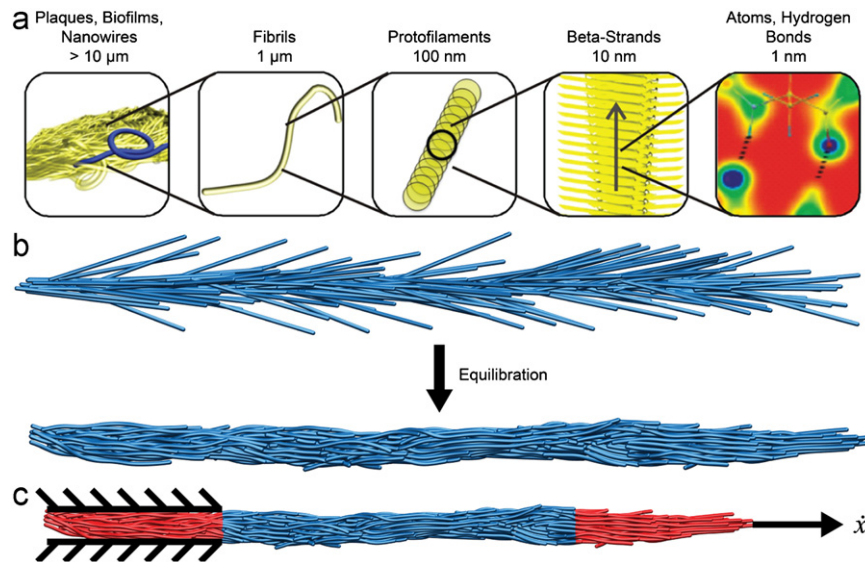


Fig. 1 – Amyloid structure and nanowire geometry. Panel (a) shows the hierarchical structure of amyloid biomaterials, displaying the range of organization from the atomic to the micrometer scale. Panel (b) shows the initial structure with randomly oriented fibrils and the nanowire structure after equilibration. Panel (c) shows a schematic of the loading conditions used. The red sections are those to which the boundary conditions are applied. The left end is held fixed and the right end is moved at a constant displacement rate. The blue section in the middle is unconstrained and free to deform. Panel (a) adapted from Knowles and Buehler, 2011. (For interpretation of the references to color in this figure legend, the reader is referred to the web version of this article.)

Two parameters are varied in order to examine the effect of the fibril properties on the response of the overall nanowire structure: the breaking strain (controlled by changing r_{break}) and the strength of the interfibril adhesion (A). The breaking strain is varied between approximately 0.8 and 2 times the nominal breaking strain (0.48%) and the adhesion strength is varied between 0.1 and 3.5 times its nominal value. In all cases an additional equilibration run is performed after varying the fibril properties to ensure that each structure starts from a stress-free configuration.

The amyloid nanowire structures are subjected to uniaxial tension to examine their mechanical properties and deformation behavior. Deformation is applied by holding one end of the nanowire fixed and moving the other end at a constant

velocity of 0.5 m s^{-1} (Fig. 1(c)); the groups of particles to which the boundary conditions are applied are each approximately 150 nm in length. During pulling, both the virial stress and the engineering strain in the unfixed section are recorded. Since the virial stress is reported as a stress-volume product, all stress values are calculated by dividing by the initial volume of the free section of the nanowire with nominal fibril properties. Furthermore, to more clearly show changes in behavior that result from varying the fibril properties, all calculations are normalized by the results from the nominal fibril property nanowire structure. Visual analysis is performed with VMD (Humphrey et al., 1996) to examine changes in deformation mechanism that result from varying the fibril properties.

3. Results and discussion

3.1. Deformation mechanism

One of the most apparent changes that the amyloid nanowire structures undergo upon varying the fibril properties is seen in the mechanism by which they deform. We note that even when varying the fibril failure strain, the individual amyloid fibrils are always quite brittle—the maximum failure strain is below 1%. However, in the nanowire structure, deformation is not limited to axial stretching and bending as it is for single fibrils. Instead, deformation is controlled by a competition between two mechanisms: sliding of fibrils passed each other and failure of individual fibrils (due to axial stretching beyond the breaking strain).

In the case of the nominal fibril properties, the nanowire displays mostly brittle behavior. While some fibril sliding is observed, the majority of the deformation is accommodated by failure of individual fibrils. As seen in Fig. 2(a), as the fibril breaking strain is increased and the individual fibrils become more resistant to failure, there is a clear transition to ductile behavior. Very little fibril failure is observed and the large amount of fibril sliding results in the nanowires exhibiting some necking before ultimately failing due to the finite length of the fibrils.

A similar transition between ductile and brittle behavior is observed upon varying the interfibril adhesion strength. For low adhesion strengths, there is little resistance to fibril sliding and the nanowires feature ductile behavior, but increasing the adhesion strength results in much more fibril failure and an overall brittle response in the nanowire (Fig. 2(b)).

3.2. Young's modulus

We next examine the effect of varying the fibril properties on the Young's modulus of the nanowire structures. To provide a consistent measure between all cases, the modulus is obtained by performing a linear fit on the stress–strain curve up to 0.05% strain. As seen in Fig. 3(a), the fibril failure strain

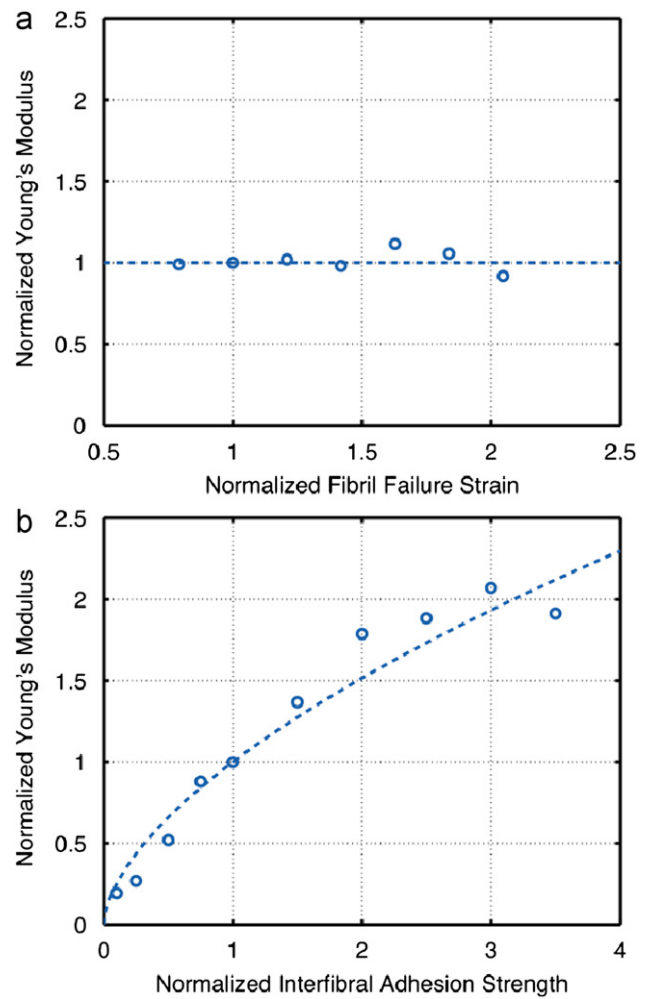


Fig. 3 – Effect of amyloid fibril properties on the Young's modulus of the nanowire structure. Panel (a) shows that varying the fibril failure strain has little effect on the modulus of the nanowire structure, while panel (b) shows that the interfibril adhesion strength strongly affects the nanowire modulus. The dashed lines in each panel qualitatively demonstrate the trends.

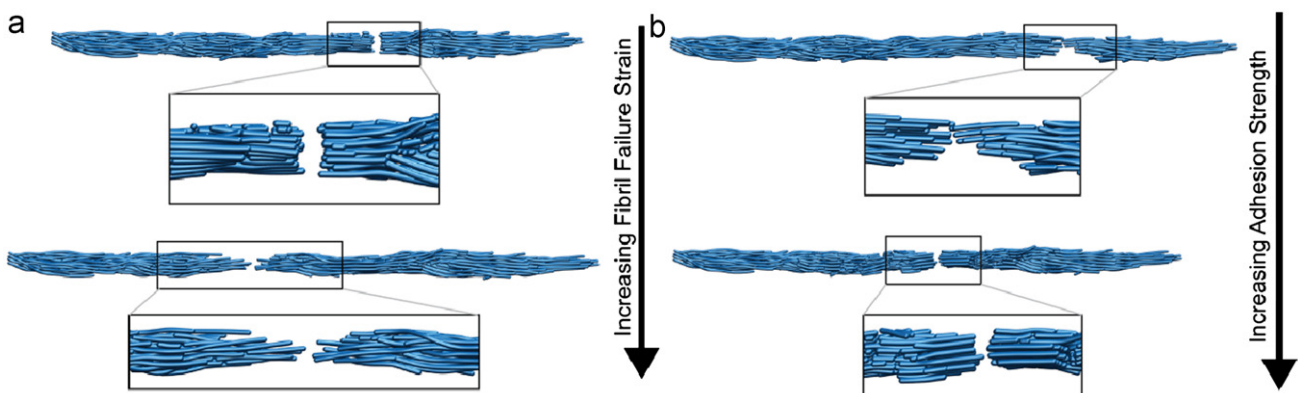


Fig. 2 – The deformation mechanisms seen in the amyloid nanowires depend strongly on the properties of the fibrils. Panel (a) shows the clear transition from brittle to ductile behavior that occurs upon increasing the fibril failure strain; the opposite trend is observed in Panel (b) upon increasing the interfibril adhesion strength. For small fibril failure strains and large interfibril adhesion strength, deformation is dominated by failure of individual fibrils and the fracture surface of nanowire is mostly flat. In contrast, for large fibril failure strains and small interfibril adhesion strength, fibril sliding is the dominant deformation mechanism and a necking behavior is seen before failure.

has little to no effect on the modulus of the nanowire. This result is not surprising; in the very small strain range from which the Young's modulus is determined, the strain in individual fibrils does not exceed the breaking strain and thus the nanowire properties remain constant.

In contrast, varying the interfibril adhesion strength has a large effect on the modulus of the nanowire (Fig. 3(b)). Increasing the adhesion strength reduces the ability of the fibrils to slide past each other and thus results in an increased stiffness. These results indicate that in the elastic regime, the mechanical response of larger scale amyloid structures is dominated by the interactions between fibrils rather than the elastic properties of the fibrils themselves.

We note that the value we find for the Young's modulus of the nanowire structure with the nominal fibril properties is 0.612 GPa, about one fourth of the modulus of an individual

fibril (in the small strain regime). This result is not surprising since the fibril sliding deformation mechanism in the nanowire allows the structure to deform without axially stretching the individual fibrils and thus significantly reduces the modulus of the larger structure.

3.3. Ultimate strength and failure strain

Fig. 4 shows how the ultimate tensile strength and failure strain of the nanowires varies with the fibril properties. As expected, increasing the fibril breaking strain allows the nanowire to achieve a higher strength and strain to failure (Fig. 4(a)). However, since the deformation mechanism shifts to one dominated by fibrils sliding past each other as described above, once the fibril breaking strain is increased sufficiently such that the fibrils will always slide out before breaking, the ultimate strength and failure strain of the nanowires are not expected to continue to increase with increasing fibril failure strain. Instead they are limited by the amount of overlap among the fibrils in the structure. Nanowires constructed from longer fibrils or with a higher linear density of fibrils would be expected to achieve higher strains before failure, but these effects are not examined in the present work.

The effect of the interfibril adhesion strength is shown in Fig. 4(b). The ultimate strength increases initially with increasing adhesion strength but levels off when the adhesion becomes too large because the strength of attraction between fibrils begins to exceed the strength of the bonds within the fibrils. This causes the fibrils to break even under small applied loads. The dramatic decrease of failure strain with increasing adhesion strength demonstrates the transition to brittle behavior and highlights the inherent tradeoff between enhanced strength and reduced ductility.

3.4. Toughness modulus

Finally, the toughness modulus of the amyloid nanowires is calculated from our *in silico* experiments to explore how varying the fibril properties affects the ability of the structures to absorb energy during deformation. Since increasing the fibril failure strain resulted in an increase in both the ultimate strength and strain to failure, it is not surprising that a large increase in the toughness modulus is also observed (Fig. 5(a)). This indicates that by finding ways to increase the failure strain of individual fibrils, structures can be created that are very mechanically robust. In contrast, the tradeoff of enhanced strength and increased brittleness with increasing interfibril adhesion strength causes the toughness modulus to remain mostly unchanged over the range of adhesion strengths studied as shown in Fig. 5(b).

More notably, the toughness modulus of an individual amyloid fibril is indicated in each plot by the dashed red line, and in almost every case the toughness modulus of the nanowire structure exceeds that of the individual fibril. For the nanowire with nominal fibril properties, the toughness modulus is almost 2.5 times the value for the single fibril. Thus the robustness of larger scale structures is not limited by the brittle nature of the constituent fibrils; the existence of new deformation mechanisms such as fibril sliding in the nanowires provides an avenue to

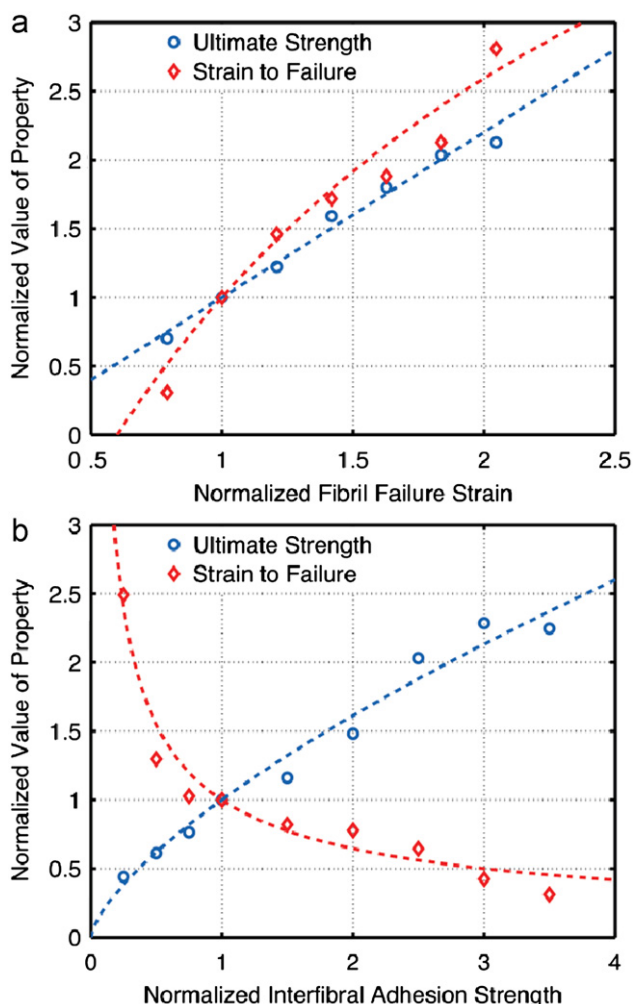


Fig. 4 – Variation of the ultimate tensile strength and strain to failure of the amyloid nanowire with the amyloid fibril properties. Panel (a) shows that increasing the failure strength of individual fibrils results in a higher ultimate strength and failure strain for the nanowire. In contrast, panel (b) demonstrates the tradeoff between enhanced strength and reduced ductility that occurs upon increasing the interfibril adhesion strength. The dashed lines in each panel qualitatively demonstrate the trends.

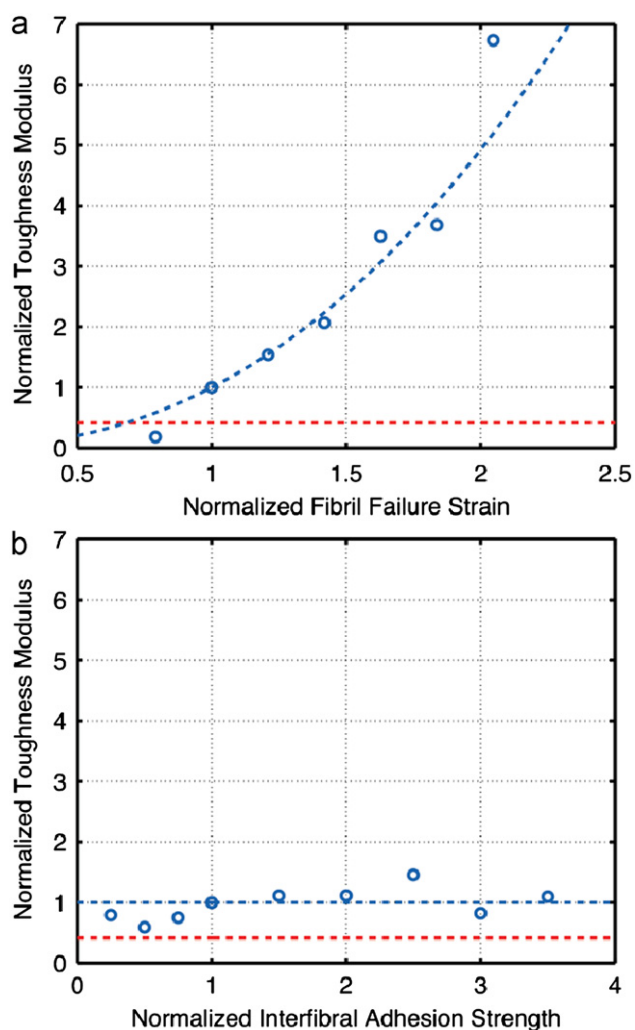


Fig. 5 – Effect of fibril properties on the toughness modulus of the amyloid nanowire structures. The dashed red line in each panel shows the toughness modulus of a single amyloid fibril. Panel (a) clearly shows that increasing the fibril failure strain results in a large increase in the toughness modulus. However, due to competition between enhanced strength and reduced strain to failure, increasing the interfibril adhesion strength has little effect on the toughness modulus as shown in panel (b). Also noteworthy is the fact that in almost every case, the larger scale amyloid nanowire has a higher toughness modulus than the individual fibrils. The dashed lines in each panel qualitatively demonstrate the trends. (For interpretation of the references to color in this figure legend, the reader is referred to the web version of this article.)

offset the brittleness of amyloid fibrils and increase their utility in large scale structures.

4. Conclusion

Our results demonstrate a clear link between the properties of individual amyloid fibrils and the mechanical behavior of larger scale structures made from them. Small changes in either the fibril breaking strain or the interfibril adhesion

strength result in dramatic changes in deformation mechanism and a transition from a rather brittle to a more ductile behavior, and changes in the mechanical properties of the nanowires are in general strongly correlated with the changing deformation mechanisms that result from varying the fibril properties. We also show that structures such as the nanowires studied in this work can be made from brittle building blocks like amyloid fibrils but still display ductility and robustness; and the emergence of new deformation mechanisms at larger length scales mitigates some of the brittleness of the individual fibrils.

The scope of our results is not limited to amyloid protein fibrils. The large increase in performance that we observe upon increasing the fibril failure strain indicates that the use of other protein structures could give better results than amyloid fibrils for different applications. For example, β -helical protein fibrils have a β -sheet rich secondary structure like amyloid fibrils, but they also possess a continuous covalently bonded backbone (Cox et al., 2005) which could allow them to reach much higher strains before failing, and thus nanowire structures made from them could have a very large toughness modulus.

The analysis presented here shows the promise of using protein based materials in the design of larger scale functional materials. We only studied one particular protein fibril— $A\beta(1-40)$ amyloid fibrils. There is much opportunity in exploring the huge space of amyloid and other fibril forming proteins to find those that give the optimal performance for various applications and allow for the development of a new class of nanomaterials.

REFERENCES

- Aguzzi, A., 2009. Beyond the prion principle. *Nature* 459, 924–925.
- Chapman, M.R., Robinson, L.S., Pinkner, J.S., Roth, R., Heuser, J., Hammar, M., Normark, S., Hultgren, S.J., 2002. Role of *Escherichia coli* curli operons in directing amyloid fiber formation. *Science* 295, 851–855.
- Chiti, F., Dobson, C.M., 2006. Protein misfolding, functional amyloid, and human disease. *The Annual Review of Biochemistry* 75, 333–366.
- Collins, S.R., Dougllass, A., Vale, R.D., Weissman, J.S., 2004. Mechanism of prion propagation: amyloid growth occurs by monomer addition. *PLoS Biology* 2, 1582–1590.
- Cox, D.L., Lashuel, H., Lee, K.Y.C., Singh, R.R.P., 2005. The materials science of protein aggregation. *MRS Bulletin* 30, 452–457.
- Dobson, C.M., 1999. Protein misfolding, evolution and disease. *Trends in Biochemical Sciences* 24, 329–332.
- Dobson, C.M., 2003. Protein folding and misfolding. *Nature* 426, 884–890.
- Fowler, D.M., Koulov, A.V., Balch, W.E., Kelly, J.W., 2007. Functional amyloid—from bacteria to humans. *Trends in Biochemical Sciences* 32, 217–224.
- Humphrey, W., Dalke, A., Schulten, K., 1996. VMD: visual molecular dynamics. *Journal of Molecular Graphics and Modelling* 14, 33–38.
- Jaroniec, C.P., MacPhee, C.E., Bajaj, V.S., McMahon, M.T., Dobson, C.M., Griffin, R.G., 2004. High-resolution molecular structure of a peptide in an amyloid fibril determined by magic angle spinning NMR spectroscopy. *Proceedings of the National Academy of Sciences of the United States of America* 101, 711–716.
- Knowles, T.P., Fitzpatrick, A.W., Meehan, S., Mott, H.R., Vendruscolo, M.E., Dobson, C.M., Welland, M.E., 2007. Role of

- intermolecular forces in defining material properties of protein nanofibrils. *Science* 318, 1900–1903.
- Knowles, T.P.J., Buehler, M.J., 2011. Nanomechanics of functional and pathological amyloid materials. *Nature Nanotechnology* 6, 469–479.
- Knowles, T.P.J., Oppenheim, T.W., Buell, A.K., Chirgadze, D.Y., Welland, M.E., 2010. Nanostructured films from hierarchical self-assembly of amyloidogenic proteins. *Nature Nanotechnology* 5, 204–207.
- Kol, N., Adler-Abramovich, L., Barlam, D., Shneck, R.Z., Gazit, E., Rouso, I., 2005. Self-assembled peptide nanotubes are uniquely rigid bioinspired supramolecular structures. *Nano Letters* 5, 1343–1346.
- Luhrs, T., Ritter, C., Adrian, M., Riek-Loher, D., Bohrmann, B., Doeli, H., Schubert, D., Riek, R., 2005. 3D structure of Alzheimer's amyloid-beta(1-42) fibrils. *Proceedings of the National Academy of Sciences of the United States of America* 102, 17342–17347.
- Maji, S.K., Perrin, M.H., Sawaya, M.R., Jessberger, S., Vadodaria, K., Rissman, R.A., Singru, P.S., Nilsson, K.P.R., Simon, R., Schubert, D., Eisenberg, D., Rivier, J., Sawchenko, P., Vale, W., Riek, R., 2009. Functional amyloids as natural storage of peptide hormones in pituitary secretory granules. *Science* 325, 328–332.
- Paparcone, R., Buehler, M.J., 2010. Failure of Alzheimer's A beta (1-40) amyloid nanofibrils under compressive loading. *The Journal of the Minerals, Metals & Materials Society (TMS)* 62, 64–68.
- Paparcone, R., Buehler, M.J., 2011. Failure of A beta(1-40) amyloid fibrils under tensile loading. *Biomaterials* 32, 3367–3374.
- Paparcone, R., Cranford, S., Buehler, M.J., 2010a. Compressive deformation of ultralong amyloid fibrils. *Acta Mechanica Sinica* 26, 977–986.
- Paparcone, R., Cranford, S.W., Buehler, M.J., 2011. Self-folding and aggregation of amyloid nanofibrils. *Nanoscale* 3, 1748–1755.
- Paparcone, R., Keten, S., Buehler, M.J., 2010b. Atomistic simulation of nanomechanical properties of Alzheimer's A beta(1-40) amyloid fibrils under compressive and tensile loading. *Journal of Biomechanics* 43, 1196–1201.
- Plimpton, S., 1995. Fast parallel algorithms for short-range molecular-dynamics. *Journal of Computational Physics* 117, 1–19.
- Pugno, N.M., 2007a. The role of defects in the design of space elevator cable: from nanotube to megatube. *Acta Materialia* 55, 5269–5279.
- Pugno, N.M., 2007b. Space elevator: out of order?. *Nano Today* 2, 44–47.
- Pugno, N.M., 2010. The design of self-collapsed super-strong nanotube bundles. *Journal of the Mechanics and Physics of Solids* 58, 1397–1410.
- Sawaya, M.R., Sambashivan, S., Nelson, R., Ivanova, M.I., Sievers, S.A., Apostol, M.I., Thompson, M.J., Balbirnie, M., Wiltzius, J.J.W., McFarlane, H.T., Madsen, A.O., Riek, C., Eisenberg, D., 2007. Atomic structures of amyloid cross-beta spines reveal varied steric zippers. *Nature* 447, 453–457.
- Shorter, J., Lindquist, S., 2006. Destruction or potentiation of different prions catalyzed by similar Hsp104 remodeling activities. *Molecular Cell* 23, 425–438.
- Smith, J.F., Knowles, T.P.J., Dobson, C.M., MacPhee, C.E., Welland, M.E., 2006. Characterization of the nanoscale properties of individual amyloid fibrils. *Proceedings of the National Academy of Sciences of the United States of America* 103, 15806–15811.
- Solar, M., Buehler, M.J., 2012. Comparative analysis of nanomechanics of protein filaments under lateral loading. *Nanoscale* 4, 1177–1183.
- Tanaka, M., Collins, S.R., Toyama, B.H., Weissman, J.S., 2006. The physical basis of how prion conformations determine strain phenotypes. *Nature* 442, 585–589.
- Xu, Z.P., Paparcone, R., Buehler, M.J., 2010. Alzheimer's A beta (1-40) amyloid fibrils feature size-dependent mechanical properties. *Biophysical Journal* 98, 2053–2062.
- Zhang, S.G., 2003. Fabrication of novel biomaterials through molecular self-assembly. *Nature Biotechnology* 21, 1171–1178.
- Zhang, S.G., Holmes, T., Lockshin, C., Rich, A., 1993. Spontaneous assembly of a self-complementary oligopeptide to form a stable macroscopic membrane. *Proceedings of the National Academy of Sciences of the United States of America* 90, 3334–3338.